Search for the reactions $e^+e^- \rightarrow \mu^+\tau^-$ and $e^+e^- \rightarrow e^+\tau^-$

B. Aubert,[1] M. Bona,[1] D. Boutigny,[1] F. Couderc,[1] Y. Karyotakis,[1] J. P. Lees,[1] V. Poireau,[1] V. Tisserand,[1] A. Zghiche,[1] E. Grauges,[2] A. Palano,[3] J. C. Chen,[4] N. D. Qi,[4] G. Rong,[4] P. Wang,[4] Y. S. Zhu,[4] G. Eigen,[5] I. Ofte,[5] B. Stugu,[5] G. S. Abrams,[6] M. Battaglia,[6] D. N. Brown,[6] J. Button-Shafer,[6] R. N. Cahn,[6] E. Charles,[6] M. S. Gill,[6] Y. Groysman,[6] R. G. Jacobsen,[6] J. A. Kadyk,[6] L. T. Kerth,[6] Yu. G. Kolomensky,[6] G. Kukartsev,[6] G. Lynch,[6] L. M. Mir,[6] T. J. Orimoto,[6] M. Pripstein,[6] N. A. Roe,[6] M. T. Ronan,[6] W. A. Wenzel,[6] P. del Amo Sanchez,[7] M. Barrett,[7] K. E. Ford,[7] A. J. Hart,[7] T. J. Harrison,[7] C. M. Hawkes,[7] A. T. Watson,[7] T. Held,[8] H. Koch,[8] B. Lewandowski,[8] M. Pelizaeus,[8] K. Peters,[8] T. Schroeder,[8] M. Steinke,[8] J. T. Boyd,[9] J. P. Burke,[9] W. N. Cottingham,[9] D. Walker,[9] D. J. Asgeirsson,[10] T. Cuhadar-Donszelmann,[10] B. G. Fulsom,[10] C. Hearty,[10] N. S. Knecht,[10] T. S. Mattison,[10] J. A. McKenna,[10] A. Khan,[11] P. Kyberd,[11] M. Saleem,[11] D. J. Sherwood,[11] L. Teodorescu,[11] V. E. Blinov,[12] A. D. Bukin,[12] V. P. Druzhinin,[12] V. B. Golubev,[12] A. P. Onuchin,[12] S. I. Serednyakov,[12] Yu. I. Skovpen,[12] E. P. Solodov,[12] K. Yu Todyshev,[12] M. Bondioli,[13] M. Bruinsma,[13] M. Chao,[13] S. Curry,[13] I. Eschrich,[13] D. Kirkby,[13] A. J. Lankford,[13] P. Lund,[13] M. Mandelkern,[13] R. K. Mommsen,[13] W. Roethel,[13] D. P. Stoker,[13] S. Abachi,[14] C. Buchanan,[14] S. D. Foulkes,[15] J. W. Gary,[15] O. Long,[15] B. C. Shen,[15] K. Wang,[15] L. Zhang,[15] H. K. Hadavand,[16] E. J. Hill,[16] H. P. Paar,[16] S. Rahatlou,[16] V. Sharma,[16] J. W. Berryhill,[17] C. Campagnari,[17] A. Cunha,[17] B. Dahmes,[17] T. M. Hong,[17] D. Kovalskyi,[17] J. D. Richman,[17] T. W. Beck,[18] A. M. Eisner,[18] C. J. Flacco,[18] C. A. Heusch,[18] J. Kroseberg,[18] W. S. Lockman,[18] G. Nesom,[18] T. Schalk,[18] B. A. Schumm,[18] A. Seiden,[18] P. Spradlin,[18] D. C. Williams,[18] M. G. Wilson,[18] J. Albert,[19] E. Chen,[19] A. Dvoretskii,[19] F. Fang,[19] D. G. Hitlin,[19] I. Narsky,[19] T. Piatenko,[19] F. C. Porter,[19] A. Ryd,[19] G. Mancinelli,[20] B. T. Meadows,[20] K. Mishra,[20] M. D. Sokoloff,[20] F. Blanc,[21] P. C. Bloom,[21] S. Chen,[21] W. T. Ford,[21] J. F. Hirschauer,[21] A. Kreisel,[21] M. Nagel,[21] U. Nauenberg,[21] A. Olivas,[21] W. O. Ruddick,[21] J. G. Smith,[21] K. A. Ulmer,[21] S. R. Wagner,[21] J. Zhang,[21] A. Chen,[22] E. A. Eckhart,[22] A. Soffer,[22] W. H. Toki,[22] R. J. Wilson,[22] F. Winklmeier,[22] Q. Zeng,[22] D. D. Altenburg,[23] E. Feltresi,[23] A. Hauke,[23] H. Jasper,[23] J. Merkel,[23] A. Petzold,[23] B. Spaan,[23] T. Brandt,[24] V. Klose,[24] H. M. Lacker,[24] W. F. Mader,[24] R. Nogowski,[24] J. Schubert,[24] K. R. Schubert,[24] R. Schwierz,[24] J. E. Sundermann,[24] A. Volk,[24] D. Bernard,[25] G. R. Bonneaud,[25] E. Latour,[25] Ch. Thiebaux,[25] M. Verderi,[25] P. J. Clark,[26] W. Gradl,[26] F. Muheim,[26] S. Playfer,[26] A. I. Robertson,[26] Y. Xie,[26] M. Andreotti,[27] D. Bettoni,[27] C. Bozzi,[27] R. Calabrese,[27] G. Cibinetto,[27] E. Luppi,[27] M. Negrini,[27] A. Petrella,[27] L. Piemontese,[27] E. Prencipe,[27] F. Anulli,[28] R. Baldini-Ferroli,[28] A. Calcaterra,[28] R. de Sangro,[28] G. Finocchiaro,[28] S. Pacetti,[28] P. Patteri,[28] I. M. Peruzzi,[28,*] M. Piccolo,[28] M. Rama,[28] A. Zallo,[28] A. Buzzo,[29] R. Contri,[29] M. Lo Vetere,[29] M. M. Macri,[29] M. R. Monge,[29] S. Passaggio,[29] C. Patrignani,[29] E. Robutti,[29] A. Santroni,[29] S. Tosi,[29] G. Brandenburg,[30] K. S. Chaisanguanthum,[30] M. Morii,[30] J. Wu,[30] R. S. Dubitzky,[31] J. Marks,[31] S. Schenk,[31] U. Uwer,[31] W. Bhimji,[32] D. A. Bowerman,[32] P. D. Dauncey,[32] U. Egede,[32] R. L. Flack,[32] J. A. Nash,[32] M. B. Nikolich,[32] W. Panduro Vazquez,[32] D. J. Bard,[33] P. K. Behera,[33] X. Chai,[33] M. J. Charles,[33] U. Mallik,[33] N. T. Meyer,[33] V. Ziegler,[33] J. Cochran,[34] H. B. Crawley,[34] L. Dong,[34] V. Eyges,[34] W. T. Meyer,[34] S. Prell,[34] E. I. Rosenberg,[34] A. E. Rubin,[34] A. V. Gritsan,[35] A. G. Denig,[36] M. Fritsch,[36] G. Schott,[36] N. Arnaud,[37] M. Davier,[37] G. Grosdidier,[37] A. Höcker,[37] F. Le Diberder,[37] V. Lepeltier,[37] A. M. Lutz,[37] A. Oyanguren,[37] S. Pruvot,[37] S. Rodier,[37] P. Roudeau,[37] M. H. Schune,[37] A. Stocchi,[37] W. F. Wang,[37] G. Wormser,[37] C. H. Cheng,[38] D. J. Lange,[38] D. M. Wright,[38] C. A. Chavez,[39] I. J. Forster,[39] J. R. Fry,[39] E. Gabathuler,[39] R. Gamet,[39] K. A. George,[39] D. E. Hutchcroft,[39] D. J. Payne,[39] K. C. Schofield,[39] C. Touramanis,[39] A. J. Bevan,[40] F. Di Lodovico,[40] W. Menges,[40] R. Sacco,[40] G. Cowan,[41] H. U. Flaecher,[41] D. A. Hopkins,[41] P. S. Jackson,[41] T. R. McMahon,[41] S. Ricciardi,[41] F. Salvatore,[41] A. C. Wren,[41] D. N. Brown,[42] C. L. Davis,[42] J. Allison,[43] N. R. Barlow,[43] R. J. Barlow,[43] Y. M. Chia,[43] C. L. Edgar,[43] G. D. Lafferty,[43] M. T. Naisbit,[43] J. C. Williams,[43] J. I. Yi,[43] C. Chen,[44] W. D. Hulsbergen,[44] A. Jawahery,[44] C. K. Lae,[44] D. A. Roberts,[44] G. Simi,[44] G. Blaylock,[45] C. Dallapiccola,[45] S. S. Hertzbach,[45] X. Li,[45] T. B. Moore,[45] S. Saremi,[45] H. Staengle,[45] R. Cowan,[46] G. Sciolla,[46] S. J. Sekula,[46] M. Spitznagel,[46] F. Taylor,[46] R. K. Yamamoto,[46] H. Kim,[47] S. E. Mclachlin,[47] P. M. Patel,[47] S. H. Robertson,[47] A. Lazzaro,[48] V. Lombardo,[48] F. Palombo,[48] J. M. Bauer,[49] L. Cremaldi,[49] V. Eschenburg,[49] R. Godang,[49] R. Kroeger,[49] D. A. Sanders,[49] D. J. Summers,[49] H. W. Zhao,[49] S. Brunet,[50] D. Côté,[50] M. Simard,[50] P. Taras,[50] F. B. Viaud,[50] H. Nicholson,[51] N. Cavallo,[52,†] G. De Nardo,[52] F. Fabozzi,[52,†] C. Gatto,[52] L. Lista,[52] D. Monorchio,[52] P. Paolucci,[52] D. Piccolo,[52] C. Sciacca,[52] M. A. Baak,[53] G. Raven,[53] H. L. Snoek,[53] C. P. Jessop,[54] J. M. LoSecco,[54] T. Allmendinger,[55] G. Benelli,[55] L. A. Corwin,[55] K. K. Gan,[55] K. Honscheid,[55] D. Hufnagel,[55] P. D. Jackson,[55] H. Kagan,[55] R. Kass,[55] A. M. Rahimi,[55] J. J. Regensburger,[55] R. Ter-Antonyan,[55] Q. K. Wong,[55] N. L. Blount,[56] J. Brau,[56] R. Frey,[56] O. Igonkina,[56] J. A. Kolb,[56] M. Lu,[56] R. Rahmat,[56] N. B. Sinev,[56] D. Strom,[56] J. Strube,[56] E. Torrence,[56] A. Gaz,[57] M. Margoni,[57] M. Morandin,[57] A. Pompili,[57] M. Posocco,[57] M. Rotondo,[57]

F. Simonetto,[57] R. Stroili,[57] C. Voci,[57] M. Benayoun,[58] H. Briand,[58] J. Chauveau,[58] P. David,[58] L. Del Buono,[58]
Ch. de la Vaissière,[58] O. Hamon,[58] B. L. Hartfiel,[58] Ph. Leruste,[58] J. Malclès,[58] J. Ocariz,[58] L. Roos,[58] G. Therin,[58]
L. Gladney,[59] M. Biasini,[60] R. Covarelli,[60] C. Angelini,[61] G. Batignani,[61] S. Bettarini,[61] F. Bucci,[61] G. Calderini,[61]
M. Carpinelli,[61] R. Cenci,[61] F. Forti,[61] M. A. Giorgi,[61] A. Lusiani,[61] G. Marchiori,[61] M. A. Mazur,[61] M. Morganti,[61]
N. Neri,[61] E. Paoloni,[61] G. Rizzo,[61] J. J. Walsh,[61] M. Haire,[62] D. Judd,[62] D. E. Wagoner,[62] J. Biesiada,[63] N. Danielson,[63]
P. Elmer,[63] Y. P. Lau,[63] C. Lu,[63] J. Olsen,[63] A. J. S. Smith,[63] A. V. Telnov,[63] F. Bellini,[64] G. Cavoto,[64] A. D'Orazio,[64]
D. del Re,[64] E. Di Marco,[64] R. Faccini,[64] F. Ferrarotto,[64] F. Ferroni,[64] M. Gaspero,[64] L. Li Gioi,[64] M. A. Mazzoni,[64]
S. Morganti,[64] G. Piredda,[64] F. Polci,[64] F. Safai Tehrani,[64] C. Voena,[64] M. Ebert,[65] H. Schröder,[65] R. Waldi,[65] T. Adye,[66]
N. De Groot,[66] B. Franek,[66] E. O. Olaiya,[66] F. F. Wilson,[66] R. Aleksan,[67] S. Emery,[67] A. Gaidot,[67] S. F. Ganzhur,[67]
G. Hamel de Monchenault,[67] W. Kozanecki,[67] M. Legendre,[67] G. Vasseur,[67] Ch. Yèche,[67] M. Zito,[67] X. R. Chen,[68]
H. Liu,[68] W. Park,[68] M. V. Purohit,[68] J. R. Wilson,[68] M. T. Allen,[69] D. Aston,[69] R. Bartoldus,[69] P. Bechtle,[69] N. Berger,[69]
R. Claus,[69] J. P. Coleman,[69] M. R. Convery,[69] M. Cristinziani,[69] J. C. Dingfelder,[69] J. Dorfan,[69] G. P. Dubois-Felsmann,[69]
D. Dujmic,[69] W. Dunwoodie,[69] R. C. Field,[69] T. Glanzman,[69] S. J. Gowdy,[69] M. T. Graham,[69] P. Grenier,[69] V. Halyo,[69]
C. Hast,[69] T. Hryn'ova,[69] W. R. Innes,[69] M. H. Kelsey,[69] P. Kim,[69] D. W. G. S. Leith,[69] S. Li,[69] S. Luitz,[69] V. Luth,[69]
H. L. Lynch,[69] D. B. MacFarlane,[69] H. Marsiske,[69] R. Messner,[69] D. R. Muller,[69] C. P. O'Grady,[69] V. E. Ozcan,[69]
A. Perazzo,[69] M. Perl,[69] T. Pulliam,[69] B. N. Ratcliff,[69] A. Roodman,[69] A. A. Salnikov,[69] R. H. Schindler,[69] J. Schwiening,[69]
A. Snyder,[69] J. Stelzer,[69] D. Su,[69] M. K. Sullivan,[69] K. Suzuki,[69] S. K. Swain,[69] J. M. Thompson,[69] J. Va'vra,[69]
N. van Bakel,[69] M. Weaver,[69] A. J. R. Weinstein,[69] W. J. Wisniewski,[69] M. Wittgen,[69] D. H. Wright,[69] A. K. Yarritu,[69]
K. Yi,[69] C. C. Young,[69] P. R. Burchat,[70] A. J. Edwards,[70] S. A. Majewski,[70] B. A. Petersen,[70] C. Roat,[70] L. Wilden,[70]
S. Ahmed,[71] M. S. Alam,[71] R. Bula,[71] J. A. Ernst,[71] V. Jain,[71] B. Pan,[71] M. A. Saeed,[71] F. R. Wappler,[71] S. B. Zain,[71]
W. Bugg,[72] M. Krishnamurthy,[72] S. M. Spanier,[72] R. Eckmann,[73] J. L. Ritchie,[73] A. Satpathy,[73] C. J. Schilling,[73]
R. F. Schwitters,[73] J. M. Izen,[74] X. C. Lou,[74] S. Ye,[74] F. Bianchi,[75] F. Gallo,[75] D. Gamba,[75] M. Bomben,[76] L. Bosisio,[76]
C. Cartaro,[76] F. Cossutti,[76] G. Della Ricca,[76] S. Dittongo,[76] L. Lanceri,[76] L. Vitale,[76] V. Azzolini,[77] N. Lopez-March,[77]
F. Martinez-Vidal,[77] Sw. Banerjee,[78] B. Bhuyan,[78] C. M. Brown,[78] D. Fortin,[78] K. Hamano,[78] R. Kowalewski,[78]
I. M. Nugent,[78] J. M. Roney,[78] R. J. Sobie,[78] J. J. Back,[79] P. F. Harrison,[79] T. E. Latham,[79] G. B. Mohanty,[79]
M. Pappagallo,[79] H. R. Band,[80] X. Chen,[80] B. Cheng,[80] S. Dasu,[80] M. Datta,[80] K. T. Flood,[80] J. J. Hollar,[80] P. E. Kutter,[80]
B. Mellado,[80] A. Mihalyi,[80] Y. Pan,[80] M. Pierini,[80] R. Prepost,[80] S. L. Wu,[80] Z. Yu,[80] and H. Neal[81]

(*BABAR* Collaboration)

[1]*Laboratoire de Physique des Particules, IN2P3/CNRS et Université de Savoie, F-74941 Annecy-Le-Vieux, France*
[2]*Universitat de Barcelona, Facultat de Fisica, Departament ECM, E-08028 Barcelona, Spain*
[3]*Università di Bari, Dipartimento di Fisica and INFN, I-70126 Bari, Italy*
[4]*Institute of High Energy Physics, Beijing 100039, China*
[5]*University of Bergen, Institute of Physics, N-5007 Bergen, Norway*
[6]*Lawrence Berkeley National Laboratory and University of California, Berkeley, California 94720, USA*
[7]*University of Birmingham, Birmingham, B15 2TT, United Kingdom*
[8]*Ruhr Universität Bochum, Institut für Experimentalphysik 1, D-44780 Bochum, Germany*
[9]*University of Bristol, Bristol BS8 1TL, United Kingdom*
[10]*University of British Columbia, Vancouver, British Columbia, Canada V6T 1Z1*
[11]*Brunel University, Uxbridge, Middlesex UB8 3PH, United Kingdom*
[12]*Budker Institute of Nuclear Physics, Novosibirsk 630090, Russia*
[13]*University of California at Irvine, Irvine, California 92697, USA*
[14]*University of California at Los Angeles, Los Angeles, California 90024, USA*
[15]*University of California at Riverside, Riverside, California 92521, USA*
[16]*University of California at San Diego, La Jolla, California 92093, USA*
[17]*University of California at Santa Barbara, Santa Barbara, California 93106, USA*
[18]*University of California at Santa Cruz, Institute for Particle Physics, Santa Cruz, California 95064, USA*
[19]*California Institute of Technology, Pasadena, California 91125, USA*
[20]*University of Cincinnati, Cincinnati, Ohio 45221, USA*
[21]*University of Colorado, Boulder, Colorado 80309, USA*
[22]*Colorado State University, Fort Collins, Colorado 80523, USA*
[23]*Universität Dortmund, Institut für Physik, D-44221 Dortmund, Germany*
[24]*Technische Universität Dresden, Institut für Kern- und Teilchenphysik, D-01062 Dresden, Germany*
[25]*Laboratoire Leprince-Ringuet, CNRS/IN2P3, Ecole Polytechnique, F-91128 Palaiseau, France*

[26]*University of Edinburgh, Edinburgh EH9 3JZ, United Kingdom*

[27]*Università di Ferrara, Dipartimento di Fisica and INFN, I-44100 Ferrara, Italy*

[28]*Laboratori Nazionali di Frascati dell'INFN, I-00044 Frascati, Italy*

[29]*Università di Genova, Dipartimento di Fisica and INFN, I-16146 Genova, Italy*

[30]*Harvard University, Cambridge, Massachusetts 02138, USA*

[31]*Universität Heidelberg, Physikalisches Institut, Philosophenweg 12, D-69120 Heidelberg, Germany*

[32]*Imperial College London, London, SW7 2AZ, United Kingdom*

[33]*University of Iowa, Iowa City, Iowa 52242, USA*

[34]*Iowa State University, Ames, Iowa 50011-3160, USA*

[35]*Johns Hopkins University, Baltimore, Maryland 21218, USA*

[36]*Universität Karlsruhe, Institut für Experimentelle Kernphysik, D-76021 Karlsruhe, Germany*

[37]*Laboratoire de l'Accélérateur Linéaire, IN2P3/CNRS et Université Paris-Sud 11,*
Centre Scientifique d'Orsay, B.P. 34, F-91898 ORSAY Cedex, France

[38]*Lawrence Livermore National Laboratory, Livermore, California 94550, USA*

[39]*University of Liverpool, Liverpool L69 7ZE, United Kingdom*

[40]*Queen Mary, University of London, E1 4NS, United Kingdom*

[41]*University of London, Royal Holloway and Bedford New College, Egham, Surrey TW20 0EX, United Kingdom*

[42]*University of Louisville, Louisville, Kentucky 40292, USA*

[43]*University of Manchester, Manchester M13 9PL, United Kingdom*

[44]*University of Maryland, College Park, Maryland 20742, USA*

[45]*University of Massachusetts, Amherst, Massachusetts 01003, USA*

[46]*Massachusetts Institute of Technology, Laboratory for Nuclear Science, Cambridge, Massachusetts 02139, USA*

[47]*McGill University, Montréal, Québec, Canada H3A 2T8*

[48]*Università di Milano, Dipartimento di Fisica and INFN, I-20133 Milano, Italy*

[49]*University of Mississippi, University, Mississippi 38677, USA*

[50]*Université de Montréal, Physique des Particules, Montréal, Québec, Canada H3C 3J7*

[51]*Mount Holyoke College, South Hadley, Massachusetts 01075, USA*

[52]*Università di Napoli Federico II, Dipartimento di Scienze Fisiche and INFN, I-80126, Napoli, Italy*

[53]*NIKHEF, National Institute for Nuclear Physics and High Energy Physics, NL-1009 DB Amsterdam, The Netherlands*

[54]*University of Notre Dame, Notre Dame, Indiana 46556, USA*

[55]*Ohio State University, Columbus, Ohio 43210, USA*

[56]*University of Oregon, Eugene, Oregon 97403, USA*

[57]*Università di Padova, Dipartimento di Fisica and INFN, I-35131 Padova, Italy*

[58]*Laboratoire de Physique Nucléaire et de Hautes Energies, IN2P3/CNRS, Université Pierre et Marie Curie-Paris6,*
Université Denis Diderot-Paris7, F-75252 Paris, France

[59]*University of Pennsylvania, Philadelphia, Pennsylvania 19104, USA*

[60]*Università di Perugia, Dipartimento di Fisica and INFN, I-06100 Perugia, Italy*

[61]*Università di Pisa, Dipartimento di Fisica, Scuola Normale Superiore and INFN, I-56127 Pisa, Italy*

[62]*Prairie View A&M University, Prairie View, Texas 77446, USA*

[63]*Princeton University, Princeton, New Jersey 08544, USA*

[64]*Università di Roma La Sapienza, Dipartimento di Fisica and INFN, I-00185 Roma, Italy*

[65]*Universität Rostock, D-18051 Rostock, Germany*

[66]*Rutherford Appleton Laboratory, Chilton, Didcot, Oxon, OX11 0QX, United Kingdom*

[67]*DSM/Dapnia, CEA/Saclay, F-91191 Gif-sur-Yvette, France*

[68]*University of South Carolina, Columbia, South Carolina 29208, USA*

[69]*Stanford Linear Accelerator Center, Stanford, California 94309, USA*

[70]*Stanford University, Stanford, California 94305-4060, USA*

[71]*State University of New York, Albany, New York 12222, USA*

[72]*University of Tennessee, Knoxville, Tennessee 37996, USA*

[73]*University of Texas at Austin, Austin, Texas 78712, USA*

[74]*University of Texas at Dallas, Richardson, Texas 75083, USA*

[75]*Università di Torino, Dipartimento di Fisica Sperimentale and INFN, I-10125 Torino, Italy*

[76]*Università di Trieste, Dipartimento di Fisica and INFN, I-34127 Trieste, Italy*

[77]*IFIC, Universitat de Valencia-CSIC, E-46071 Valencia, Spain*

[78]*University of Victoria, Victoria, British Columbia, Canada V8W 3P6*

[79]*Department of Physics, University of Warwick, Coventry CV4 7AL, United Kingdom*

[80]*University of Wisconsin, Madison, Wisconsin 53706, USA*

[81]*Yale University, New Haven, Connecticut 06511, USA*

We report on a search for the lepton-flavor-violating processes $e^+e^- \to \mu^+\tau^-$ and $e^+e^- \to e^+\tau^-$. The data sample corresponds to an integrated luminosity of 211 fb^{-1} recorded by the *BABAR* experiment at the SLAC PEP-II asymmetric-energy *B* Factory at a center-of-mass energy of $\sqrt{s} = 10.58$ GeV. We find no evidence for a signal and set the 90% confidence level upper limits on the cross sections to be $\sigma_{\mu\tau} <$ 3.8 fb and $\sigma_{e\tau} < 9.2$ fb. The ratio of the cross sections with respect to the dimuon cross section are measured to be $\sigma_{\mu\tau}/\sigma_{\mu\mu} < 3.4 \times 10^{-6}$ and $\sigma_{e\tau}/\sigma_{\mu\mu} < 8.2 \times 10^{-6}$.

Within the standard model (SM), the fermion mass matrices and the mechanism of electroweak symmetry breaking remain unexplained. Lepton-flavor is not a conserved quantity protected by an established gauge principle. Extensions to the SM which include our knowledge of neutrino masses and mixing [1] predict lepton-flavor-violation (LFV) at a level many orders of magnitude below the current experimental sensitivity [2].

Searches for LFV have primarily concentrated on the decay of the lepton. Limits in a number of muon decay channels have reached the 10^{-11}–10^{-12} level [3] while recent measurements of LFV in tau decays have placed limits on the branching fractions $\mathcal{B}(\tau^\pm \to \mu^\pm\gamma) < 6.8 \times 10^{-8}$ and $\mathcal{B}(\tau^\pm \to e^\pm\gamma) < 1.1 \times 10^{-7}$ [4] at the 90% confidence level (CL).

There are theories that suggest lepton-flavor can be conserved in lepton decay but still be present in production. Some of these models allow for channels such as $e^+e^- \to \mu^+\tau^-$ and $e^+e^- \to e^+\tau^-$ through the Q^2 evolution of the off-diagonal elements of the fermion mass matrices [5]. Experimental limits on LFV in production are considerably weaker than for decay. At center-of-mass (CM) energies, $\sqrt{s} = 29$ GeV, there are limits on the cross section ratios $\sigma_{\mu\tau}/\sigma_{\mu\mu} < 6.1 \times 10^{-3}$ and $\sigma_{e\tau}/\sigma_{\mu\mu} < 1.8 \times 10^{-3}$ (95% CL) [6]; at $\sqrt{s} = 92$ GeV, where Z^0 exchange dominates, $\mathcal{B}(Z^0 \to \mu\tau, e\tau) < \mathcal{O}(1) \times 10^{-5}$ (95% CL) [7]. The best limits from searches at LEP energies above the Z^0 peak are $\sigma_{\mu\tau} < 64$ fb and $\sigma_{e\tau} < 78$ fb (95% CL) [8]. No equivalent measurements exist at the lower energies accessible by the *BABAR* detector.

We present results on two modes of the process $e^+e^- \to l^+\tau^-$, where l^+ is an electron or muon and the τ^- decays either to $\pi^-\pi^+\pi^-\nu_\tau$ or $\pi^-\nu_\tau$, using data recorded by the *BABAR* detector at the SLAC PEP-II asymmetric-energy e^+e^- storage rings. Inclusion of the charge-conjugate reaction $e^+e^- \to l^-\tau^+$ is assumed throughout this paper. The data sample corresponds to an integrated luminosity of $\mathcal{L} = 211$ fb^{-1} recorded at a CM energy of $\sqrt{s} = 10.58$ GeV.

The *BABAR* detector is described in detail in Ref. [9]. Charged particles are reconstructed as tracks with a 5-layer silicon vertex tracker and a 40-layer drift chamber (DCH) inside a 1.5 T solenoidal magnet. An electromagnetic calorimeter (EMC) is used to identify electrons and photons. A ring-imaging Cherenkov detector (DIRC) is used to identify charged hadrons and provides additional electron

identification information. Muons are identified by an instrumented magnetic-flux return (IFR).

Monte Carlo (MC) simulation is used to evaluate the background contamination and selection efficiency. The simulated backgrounds are also used to cross-check the selection optimization procedure and for studies of systematic effects; however, the final background yield estimation relies solely on data. The signal $e^+e^- \to l^-\tau^+$ channels are simulated using EvtGen [10] in which photon radiation is handled by the PHOTOS package [11] to an accuracy better than 1%. The background τ-pair events are simulated using the KK2F MC generator [12]. The τ decays are modeled with Tauola [13] according to measured rates with the decay $\tau^- \to \pi^-\pi^+\pi^-\nu_\tau$ assuming an intermediate $a_1^-(1260)$ axial-vector state [3,14]. We also generate light quark continuum events ($e^+e^- \to q\bar{q}$, $q = u, d, s$), charm, dimuon, Bhabhas, $B\bar{B}$, and two-photon events [10,15]. The detector response is simulated with GEANT4 [16] and all simulated events are reconstructed in the same manner as data.

The signature of the signal process in the CM frame is an isolated high-momentum muon or electron recoiling against either one or three charged pions and no neutral particles. The reconstructed mass of the missing neutrino should be consistent with a massless particle and the invariant mass of the recoiling pions and neutrino consistent with that of the τ.

We search for events with zero total charge and either two or four well-measured charged tracks originating from the e^+e^- interaction region. All charged tracks must be isolated from neutral energy deposits in the EMC and be within the acceptance of the EMC, DIRC, and IFR to ensure good particle identification. One track must be identified as either an electron or muon with a CM momentum greater than 4.68 GeV/c and no other track identified as a kaon or lepton. The electron momentum is corrected for energy loss from Bremsstrahlung emission by including in the electron momentum the energies of isolated calorimeter deposits consistent with a photon within a cone of radius 0.1 rad around the initial track momentum vector.

In the CM system, the event topology must be consistent with an e^+/μ^+ recoiling against the remaining tracks. We calculate the thrust axis [17] using all the charged and neutral deposits in the event and define two hemispheres with respect to the plane normal to the thrust axis and

require that the e^+/μ^+ and the other tracks be in separate hemispheres.

The τ has a fixed CM energy and momentum:

$$E_\tau^* = \frac{\sqrt{s}}{2} + \frac{(M_\tau^2 - M_l^2)}{2\sqrt{s}}, \qquad |\mathbf{p}_\tau^*| = \sqrt{E_\tau^{*2} - M_\tau^2}, \quad (1)$$

where M_τ and M_l are the masses of the τ and e^+/μ^+, respectively [3]. We define the direction of the τ as opposite to that of the e^+/μ^+ and assign it the momentum from Eq. (1). The CM four-momentum of the missing neutrino from the τ decay, p_ν^*, is defined as $p_\tau^* - p_\pi^*$, where p_π^* is the sum of the CM four-momenta of the pions. The reconstructed τ mass is defined to be $m_\tau = \sqrt{(E_\pi^* + |\mathbf{p}_\nu^*|)^2 - |\mathbf{p}_\tau^*|^2}$ where E_π^* is the CM energy of the pions.

Events are rejected if the quantity ΔE, the difference between the e^+/μ^+ CM energy and $\sqrt{s}/2$, is less than -0.5 GeV or greater than 0.2 GeV. True signal events will have $\Delta E \sim -0.15$ GeV while $e^+e^- \rightarrow \mu^+\mu^-$ or $e^+e^- \rightarrow e^+e^-$ events will peak at zero and $e^+e^- \rightarrow \tau^+\tau^-$ background events have large negative ΔE. The ΔE resolution is approximately 50 MeV. Events with converted photons are also rejected, where a converted photon is defined to be a pair of oppositely charged tracks assumed to have the electron mass and coming from a vertex with a combined mass less than 150 MeV/c^2.

We use a number of kinematic variables to suppress backgrounds. The missing event energy in the CM frame, $E_{\rm miss}^*$, defined as the difference between $\sqrt{s}$ and the sum of the charged track energies, is distributed uniformly for signal but peaks at zero or near $\sqrt{s}/2$ for the most important backgrounds. The missing mass squared, $m_{\rm miss}^2$, should be consistent with zero. A requirement on the maximum neutral energy cluster in the detector, E_γ, eliminates events with neutral pions or photons [18]. A requirement on the angle in the CM between the direction of the neutrino and the beam axis in the e^- beam direction, $\cos^*(\theta_\nu)$, ensures the reconstructed neutrino is within the detector acceptance to reject events with significant radiation along the beam direction. The angle in the CM between the direction of the neutrino and the τ, $\theta_{\tau\nu}^*$, is used to reject background events with a back-to-back track topology such as dimuon and Bhabha production. An event is accepted if it falls within a two-dimensional region defined with respect to m_τ and the e^+/μ^+ CM momentum, p_l^*. Events in this region are then used in a maximum likelihood fit to extract the signal yield.

The values of the selection criteria are shown in Table I. We optimize the selection sensitivity by defining a nominal signal box with a width of 3 standard deviations in the reconstructed m_τ and p_l^*. The resolutions on m_τ and p_l^* are approximately 10 MeV/c^2 and 45 MeV/c, respectively. The values of the selection criteria are chosen to maximize the discriminant $S/\sqrt{B}$ where S is the number of MC signal events in the nominal signal box and B is the number of data events accepted outside this region but within $1.5 < m_\tau < 2.2$ GeV/c^2 and the p_l^* boundaries given in Table I. We repeated the procedure using background MC within the nominal signal box instead of data and this produced consistent results. The signal MC reconstruction efficiencies and their statistical error after the application of these selection criteria are shown in Table II.

The backgrounds are dominated by $e^+e^- \rightarrow \tau^+\tau^-$ decays where one τ decays to an e^+/μ^+ plus neutrinos and the other to either $\pi^-\pi^+\pi^-\nu_\tau$ or $\pi^-\nu_\tau$. Light quark continuum processes are predicted to contribute significantly to $e^+e^- \rightarrow \mu^+\tau^-(\tau^- \rightarrow \pi^-\pi^+\pi^-\nu_\tau)$ only and events from $e^+e^- \rightarrow \mu^+\mu^-$ are only present in $e^+e^- \rightarrow \mu^+\tau^-(\tau^- \rightarrow \pi^-\nu_\tau)$. Charm and $B\bar{B}$ backgrounds are eliminated by the track multiplicity and ΔE requirement and all other backgrounds are negligible.

An extended unbinned maximum likelihood (ML) fit to the variables m_τ and p_l^* is used to extract the total number of signal and background events separately for each mode. The likelihood function L is:

$$L = \frac{e^{-\sum_j^{n_j}}}{N!} \prod_i^N \sum_j n_j \mathcal{P}_j(\vec{x}_i), \qquad (2)$$

where n_j is the yield of events of hypothesis j (signal or background) and N is the number of events in the sample. The individual background components comprise $e^+e^- \rightarrow \tau^+\tau^-$, $e^+e^- \rightarrow \mu^+\mu^-(\gamma)$, and light quark continuum decay modes. $\mathcal{P}_j(\vec{x}_i)$ is the corresponding probability density function (PDF), evaluated with the variables $\vec{x}_i = \{m_\tau, p_l^*\}$ for the ith event. For the signal, we use double Crystal Ball

TABLE I. Selection criteria for the decay modes. The same criteria are used for the e^+ and μ^+ lepton flavors except for $E_{\rm miss}^*$.

	$e^+e^- \rightarrow l^+\tau^-$ $\tau^- \rightarrow \pi^-\pi^+\pi^-\nu_\tau$			$e^+e^- \rightarrow \mu^+\tau^-$ $(e^+\tau^-)$ $\tau^- \rightarrow \pi^-\nu_\tau$		
$E_{\rm miss}^*$ (GeV)	0.015	$-$	3.23	0.65	$-$	4.55 (4.0)
$m_{\rm miss}^2$ (GeV^2/c^4)		$<$	0.56		$<$	0.65
E_γ (GeV)		$<$	0.20		$<$	0.15
$\cos^*(\theta_\nu)$	-0.9	$-$	0.9	-0.9	$-$	0.7
$\theta_{\tau\nu}^*$		$>$	0.015		$>$	0.090
m_τ (GeV/c^2)	1.6	$-$	2.0	1.6	$-$	2.0
p_l^* (GeV/c)	4.90	$-$	5.32	5.02	$-$	5.32

TABLE II. Summary of the signal yields, cross sections, and ratios of cross sections to dimuon cross section. The first uncertainty is the statistical error and the second systematic.

$e^+e^- \to \mu^+\tau^-$	$\tau^- \to \pi^-\pi^+\pi^-\nu_\tau$	$\tau^- \to \pi^-\nu_\tau$
Total events	905	575
Signal events	$-1.37 \pm 9.9 \pm 2.6$	$1.9 \pm 10.1 \pm 4.4$
Signal events (90% CL)	<19.2	<19.9
MC efficiency (%)	18.5 ± 0.2	9.62 ± 0.14
$\sigma_{\mu\tau}$ (fb)	$-0.35 \pm 2.6 \pm 0.7$	$0.85 \pm 4.5 \pm 2.0$
$\sigma_{\mu\tau}$ (90% CL)	<4.9 fb	<8.9 fb
$\sigma_{\mu\tau}$ (95% CL)	<5.91 fb	<11.4 fb
$\sigma_{\mu\tau}/\sigma_{\mu\mu}$ (90% CL)	$<4.3 \times 10^{-6}$	$<7.9 \times 10^{-6}$
$\sigma_{\mu\tau}/\sigma_{\mu\mu}$ (95% CL)	$<5.2 \times 10^{-6}$	$<10.1 \times 10^{-6}$

$e^+e^- \to e^+\tau^-$	$\tau^- \to \pi^-\pi^+\pi^-\nu_\tau$	$\tau^- \to \pi^-\nu_\tau$
Total events	537	332
Signal events	$15.9 \pm 10.3 \pm 2.7$	$10.7 \pm 8.8 \pm 2.7$
Signal events (90% CL)	<32.3	<25.8
MC efficiency (%)	11.73 ± 0.15	11.9 ± 0.15
$\sigma_{e\tau}$ (fb)	$6.5 \pm 4.2 \pm 1.1$	$3.9 \pm 3.2 \pm 1.0$
$\sigma_{e\tau}$ (90% CL)	<13.2 fb	<9.4 fb
$\sigma_{e\tau}$ (95% CL)	<14.8 fb	<11.1 fb
$\sigma_{e\tau}/\sigma_{\mu\mu}$ (90% CL)	$<11.7 \times 10^{-6}$	$<8.4 \times 10^{-6}$
$\sigma_{e\tau}/\sigma_{\mu\mu}$ (95% CL)	$<13.1 \times 10^{-6}$	$<9.8 \times 10^{-6}$

functions [19] for both m_τ and p_l^*. Because of correlations between m_τ and p_l^* for nonsignal events, we use a two-dimensional nonparametric PDF obtained from MC for the backgrounds [20]. In the maximum likelihood fit to the data, the parameters of the PDFs are fixed to the values determined from MC and only the signal and the background component yields are allowed to float. The statistical errors on the yields by the ML fit are roughly a factor of 2 smaller than those achievable with a simple counting experiment.

We check the robustness of the fitting procedure against variations in the signal size and background shape. We first fit the data outside the signal region with the MC background PDFs only, to determine their amplitudes. Using these PDFs for the background, we generate trial distributions including a Poisson-distributed number of simulated signal events, and perform the fit for each. We use 1000 trials at each of 20 values of the average signal yield between 0 and 100 events, and find the fitted signal yield to be unbiased and the statistical uncertainty to be estimated correctly. Second, we generate a set of trial distributions in which the relative amplitudes of the simulated background components are changed, and confirm that this does not bias the fitted signal yield.

As a validation check, we compare the predicted MC background levels and distributions of the variables from Table I to the data in the region outside the nominal signal box and find that they are in agreement. We also extrapolate the fitted background PDFs from the region outside the nominal signal region into the nominal signal region and predict (measure) $193 \pm 9(202)$ and $143 \pm 7(154)$ for $e^+e^- \to \mu^+\tau^-(\tau^- \to \pi^-\pi^+\pi^-\nu_\tau)$ and $e^+e^- \to \mu^+\tau^-(\tau^- \to \pi^-\nu_\tau)$, respectively, and $112 \pm 7(128)$ and $90 \pm 6(75)$ events for $e^+e^- \to e^+\tau^-(\tau^- \to \pi^-\pi^+\pi^-\nu_\tau)$ and $e^+e^- \to e^+\tau^-(\tau^- \to \pi^-\nu_\tau)$, respectively, where the error is statistical only. The predicted and measured values are consistent within the statistical errors.

From the reconstructed MC efficiency, we can estimate the predicted number of background events and compare to the results of the ML fit. For $e^+e^- \to \tau^+\tau^-$, the predicted (ML fitted) background in the fitted region is 750 ± 43 (775 ± 19) and 494 ± 40 (385 ± 35) events for $e^+e^- \to \mu^+\tau^-(\tau^- \to \pi^-\pi^+\pi^-\nu_\tau)$ and $e^+e^- \to \mu^+\tau^-(\tau^- \to \pi^-\nu_\tau)$, respectively, and 414 ± 41 (518 ± 41) and 319 ± 45 (331 ± 18) events for $e^+e^- \to e^+\tau^-(\tau^- \to \pi^-\pi^+\pi^-\nu_\tau)$ and $e^+e^- \to e^+\tau^-(\tau^- \to \pi^-\nu_\tau)$, respectively. The dimuon background to $e^+e^- \to \mu^+\tau^-(\tau^- \to \pi^-\nu_\tau)$ is predicted (ML fitted) to be 114 ± 38 (189 ± 30). For the light continuum background, the MC predicts (ML fitted) 119 ± 24 (129 ± 40) and 19 ± 9 (18 ± 35) events for $e^+e^- \to \mu^+\tau^-(\tau^- \to \pi^-\pi^+\pi^-\nu_\tau)$ and $e^+e^- \to e^+\tau^-(\tau^- \to \pi^-\pi^+\pi^-\nu_\tau)$, respectively. The predicted and fitted values agree within errors.

The main sources of systematic error on the signal yield come from uncertainties in the reconstruction, the $\tau^- \to \pi^-\pi^+\pi^-\nu_\tau$ decay mechanism, and the fit procedure. A relative systematic uncertainty of 0.8% per track, added linearly for all charged tracks in the event, is applied to account for differences in MC and data charged particle reconstruction. A relative systematic uncertainty of 1.0% per charged pion track and 1.3% per e^+/μ^+ track, added linearly for each charged track, is applied to account for differences in MC and data particle identification efficiencies.

A possible nonaxial-vector decay mechanism for the decay $\tau^- \to \pi^-\pi^+\pi^-\nu_\tau$ is not completely ruled out by current measurements [3]. To estimate this effect, the signal MC events were generated with 90% axial-vector and 10% phase-space decays and the difference in the reconstruction efficiency compared to 100% $a_1^-(1260)$ decays applied as a systematic. This introduces a relative systematic uncertainty of 3.2%.

The largest systematic error comes from the variation of the PDF fit parameters within their fitted errors. The two-dimensional nonparametric background PDFs show small structures that depend on MC statistics and the value of the smoothing parameter used [20]. By varying the smoothing parameter, using different functional forms and varying the fitted parameters within their uncertainties, we derive a systematic error of ~0.5 events. To investigate possible mismodeling of the detector acceptance and response, we repeat the analysis with each selection criterion varied by the resolution on the corresponding variable. All changes to the signal yield are smaller than the statistical error and

we conservatively take the largest change in each case as a systematic uncertainty, which ranges from 2.5 to 4.4 events. The total systematic error is between 2.6 and 4.4 events and our final limit on the cross sections is dominated by the statistical error which is of the order of 10 events.

The m_τ and p_l^* distributions for the modes are shown in Fig. 1 and the projections are shown in Figs. 2 and 3. The projection of the signal PDF is shown as the dashed line, the background PDFs as the dotted line, and the total PDF as the solid line. The central value of the cross section for $e^+e^- \rightarrow l^+\tau^-$ is given by $\sigma = N/\eta\epsilon\mathcal{L}$ where N is the number of signal events, η the signal reconstruction efficiency, and ϵ is the $\tau^- \rightarrow \pi^-\pi^+\pi^-\nu_\tau$ or $\tau^- \rightarrow \pi^-\nu_\tau$ branching fraction. The measurements are not statistically different from the null hypothesis and we obtain 90% CL upper limits by finding the maximum number of signal events N such that the integral of the total likelihood function is 90% of the total integral. From MC studies [12], the total cross section of the process $e^+e^- \rightarrow \mu^+\mu^-$ at $\sqrt{s} = 10.58$ GeV is $\sigma_{\mu\mu} = (1.13 \pm 0.02)$ nb and we use this to calculate 90% CL upper limits on the ratio of the cross sections with respect to the dimuon cross section. The central values of the signal yields from the maximum likelihood fit and the upper limits on the cross sections and cross section ratios are given in Table II.

We combine the $\tau^- \rightarrow \pi^-\pi^+\pi^-\nu_\tau$ and $\tau^- \rightarrow \pi^-\nu_\tau$ decays and calculate 90% CL upper limits on the cross sections of $\sigma_{\mu\tau} < 3.8$ fb for $e^+e^- \rightarrow \mu^+\tau^-$ and $\sigma_{e\tau} < 9.2$ fb for $e^+e^- \rightarrow e^+\tau^-$. The 90% CL upper limits on the ratio of the cross sections with respect to the dimuon cross section are calculated to be $\sigma_{\mu\tau}/\sigma_{\mu\mu} < 3.4 \times 10^{-6}$ and $\sigma_{e\tau}/\sigma_{\mu\mu} < 8.2 \times 10^{-6}$. For comparison with previous LEP results measured at $\sqrt{s} \geq 92$ GeV, the 95% CL upper limits on the cross sections and ratio of cross sections are 4.6 fb and 4.0×10^{-6} for $e^+e^- \rightarrow \mu^+\tau^-$ and 10.1 fb and 8.9×10^{-6} for $e^+e^- \rightarrow e^+\tau^-$, respectively.

FIG. 2 (color online). Reconstructed distributions for $e^+e^- \rightarrow \mu^+\tau^-$ candidates: (a) m_τ and (b) p_μ^* for $\tau^- \rightarrow \pi^-\pi^+\pi^-\nu_\tau$; and (c) m_τ and (d) p_μ^* for $\tau^- \rightarrow \pi^-\nu_\tau$. The projection of the ML fit (solid line) hides the background component (dotted line). The projection of the few signal events is shown on the horizontal axis as a dashed line. The peaking dotted line shows the expected MC signal distribution at the 90% CL upper limit.

In conclusion, we have performed the first search at a CM energy of $\sqrt{s} = 10.58$ GeV of the lepton-flavor-violating production processes $e^+e^- \rightarrow \mu^+\tau^-$ and $e^+e^- \rightarrow e^+\tau^-$. No statistically significant signal events were observed in any of the decay modes. Upper limits have been placed on the cross sections and ratios of cross sections to the dimuon cross section to form limits on $e^+e^- \rightarrow \mu^+\tau^-$ and $e^+e^- \rightarrow e^+\tau^-$.
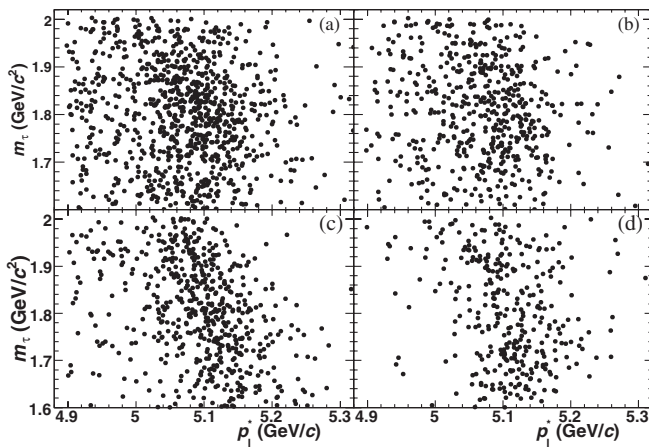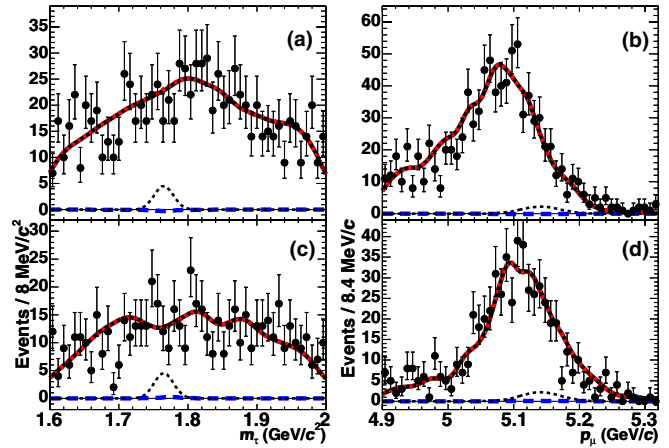
FIG. 1. m_τ versus p_l^* for reconstructed candidates for: (a) $e^+e^- \rightarrow \mu^+\tau^-(\tau^- \rightarrow \pi^-\pi^+\pi^-\nu_\tau)$; (b) $e^+e^- \rightarrow \mu^+\tau^-(\tau^- \rightarrow \pi^-\nu_\tau)$; (c) $e^+e^- \rightarrow e^+\tau^-(\tau^- \rightarrow \pi^-\pi^+\pi^-\nu_\tau)$; and (d) $e^+e^- \rightarrow e^+\tau^-(\tau^- \rightarrow \pi^-\nu_\tau)$.
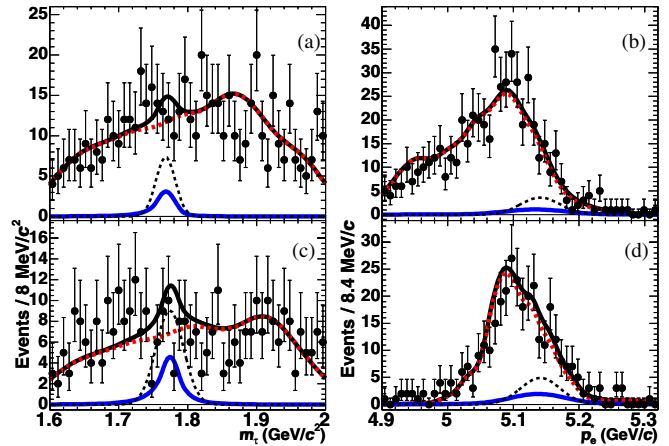

FIG. 3 (color online). Reconstructed distributions for $e^+e^- \rightarrow e^+\tau^-$ candidates: (a) m_τ and (b) p_e^* for $\tau^- \rightarrow \pi^-\pi^+\pi^-\nu_\tau$; and (c) m_τ and (d) p_e^* for $\tau^- \rightarrow \pi^-\nu_\tau$. The solid line is the projection of the ML fit, the dotted line is the background component, and the dashed line is the signal component. The peaking dotted line shows the expected MC signal distribution at the 90% CL upper limit.

[1] B. T. Cleveland *et al.* (Homestake Collaboration), Astrophys. J. **496**, 505 (1998); Y. Fukuda *et al.* (Super-Kamiokande Collaboration), Phys. Rev. Lett. **81**, 1562 (1998); Q. R. Ahmad *et al.* (SNO Collaboration), Phys. Rev. Lett. **89**, 011301 (2002).

[2] E. Ma, Nucl. Phys. B, Proc. Suppl. **123**, 125 (2003).

[3] S. Eidelman *et al.* (Particle Data Group), Phys. Lett. B **592**, 1 (2004).

[4] B. Aubert *et al.* (*BABAR* Collaboration), Phys. Rev. Lett. **95**, 041802 (2005); **96**, 041801 (2006).

[5] J. Bordes, H.-M. Chan, and S. T. Tsou, hep-ph/0111175; Phys. Rev. D **65**, 093006 (2002); Eur. Phys. J. C **27**, 189 (2003).

[6] J. J. Gomez-Cadenas *et al.* (MARK II Collaboration), Phys. Rev. Lett. **66**, 1007 (1991).

[7] M. Z. Akrawy *et al.* (OPAL Collaboration), Phys. Lett. B **254**, 293 (1991); D. Decamp *et al.* (ALEPH Collaboration), Phys. Rep. **216**, 253 (1992); P. Abreu *et al.* (DELPHI Collaboration), Phys. Lett. B **298**, 247 (1993); O. Adriani *et al.* (L3 Collaboration), Phys. Lett. B **316**, 427 (1993).

[8] G. Abbiendi *et al.* (OPAL Collaboration), Phys. Lett. B **519**, 23 (2001).

[9] B. Aubert *et al.* (*BABAR* Collaboration), Nucl. Instrum. Methods Phys. Res., Sect. A **479**, 1 (2002).

[10] D. J. Lange, Nucl. Instrum. Methods Phys. Res., Sect. A **462**, 152 (2001).

[11] E. Barberio and Z. Was, Comput. Phys. Commun. **79**, 291 (1994).

[12] S. Jadach and Z. Was, Comput. Phys. Commun. **85**, 453 (1995).

[13] S. Jadach, Z. Was, R. Decker, and J. H. Kuhn, Comput. Phys. Commun. **76**, 361 (1993).

[14] R. A. Briere *et al.* (CLEO Collaboration), Phys. Rev. Lett. **90**, 181802 (2003).

[15] B. F. Ward, S. Jadach, and Z. Was, Nucl. Phys. B, Proc. Suppl. **116**, 73 (2003); T. Sjöstrand, Comput. Phys. Commun. **82**, 74 (1994).

[16] S. Agostinelli *et al.* (GEANT4 Collaboration), Nucl. Instrum. Methods Phys. Res., Sect. A **506**, 250 (2003).

[17] S. Brandt *et al.*, Phys. Lett. **12**, 57 (1964); E. Fahri, Phys. Rev. Lett. **39**, 1587 (1977).

[18] B. Aubert *et al.* (*BABAR* Collaboration), Phys. Rev. D **73**, 057101 (2006).

[19] T. Skwarnicki, Ph.D. thesis, Cracow Institute of Nuclear Physics [DESY, Report No. DESY-F31-86-02, 1986].

[20] K. Cranmer, Comput. Phys. Commun. **136**, 198 (2001).